Proceedings of the 40th IEEE
Conference on Decision and Control
Orlando, Florida USA, December 2001

System Identification Using Subband Signal Processing

Damian Marelli and Minyue Fu
Department of Electrical and Computer Engineering
University of Newcastle, N.S.W. 2308 Australia

Abstract

The purpose of this paper is of twofold. First, we give a tutorial on a new approach to system identification using subband signal processing. Secondly, we study two types of subband identification schemes, one using critical sampling and one using over-sampling. We compare the behavior of the subband identification technique with the traditional "full-band" identification technique in terms of the computational cost, asymptotic residual error and convergence rate. This comparison is used to demonstrate the potential power of the subband technique. We also consider design issues for subband identification, especially for the case with over-sampling.

1 Introduction

The theory of linear system identification is well developed. Many references are available on the subject; see, e.g., [1, 2]. Identification algorithms based on the least-squares technique are commonly employed in practice and their behaviors are well understood. However, the direct use of this algorithm is unsuitable for real-time applications where high order finite impulse response (FIR) models are required (e.g. speech echo cancellation and channel equalization).

To alleviate the computational problem, the so-called subband identification technique has been proposed; see, e.g., [3, 4]. Loosely speaking, the subband approach divides the input and output signals into a number of subbands using two analysis filterbanks, respectively. Each analysis filterbank consist of a bank of M filters whose output is downsampled by a factor of D (i.e. one out of D samples is kept). Then for each subband channel, a subband model is identified. These subband models can be combined to give a full-band model. In many applications, the subband models are used directly to estimate certain subband signals which are combined using a synthesis filterbank to form a required signal estimate.

An example of such applications is speech echo cancellation. The reverberation model for a typical video conferencing room requires a tap size in the order of 500-1000 or more. A training signal is often available for estimating the reveberation model. Estimating a full-band model may be very computationally involved, not mentioning the numerical stability issues. In this case, subband models of reverberations can be estimated using more a numerically efficient subband identification algorithm. These models can then be used to give an estimate of the source signal (i.e., the speech signal without reverberation) in each subband. Finally, these subband signals are combined to give an estimate of the (full-band) source signal.

Another application where the subband identification technique can be used is broadband wireless channel equalization. Othorgonal frequency division multiplexing is a preferred modulation technique. This involves using a possibly large number of equally-spaced subcarriers to modulate transmit signals. The communication channel involves many (slowly time-varying) multipaths. One main difficulty with broadband wireless equalization is that the multipath channel model may require a large tap size, mainly due to the high data rate. Again, the subband identification can be used to solve this problem. There is an extra advantage of the subband technique in this application because the subband signals (i.e., the subcarrier signals) are readily available at the receiver. As we will see that this advantage yields a major computational saving.

The purpose of this paper is of twofold: First, we give a tutorial to the subband identification approach. We will show why this approach can be more numerically efficient than the full-band approach for applications where a high order model is required. Secondly, we study two types of subband identification schemes, one using critical sampling and one using over-sampling. Critical sampling refers to the case where the number of subbands is equal to the down-sampling rate, whereas in the over-sampling case the number of subbands is more than the down-sampling rate. The former case is simpler to use and easier to understand, whereas the latter case involves more design problems but give further computational savings. We compare the behavior of the subband identification technique with the traditional "full-band" identification technique in terms of the computational cost, asymptotic residual error and convergence rate. This comparison is used to demonstrate the potential power of the subband technique. We also consider design issues for subband identification, especially for the case with over-sampling. We will also give an example to illustrate the performance of the subband identification

0-7803-7061-9/01/$10.00 © 2001 IEEE

technique.

2 Review of Fullband Identification

The standard full-band identification technique is depicted in figure 1. Here, the signals $u(t), v(t)$ are assumed to be zero-mean, uncorrelated random processes, the plant $g(z)$ is a linear time-invariant system, the model $\hat{g}(z)$ is an FIR model of order n_f. We consider the prediction error method for formulation of the identification problem. More specifically, if we express the model as $\hat{g}(q) = \hat{g}(q, \hat{\theta}_t)$, where q is the forward shift operator (i.e. $qx(t) = x(t+1)$) and $\hat{g}(q, \theta)$ is a parametric model on the parameters θ, then, the optimal vector of parameters up to time t (i.e. $\hat{\theta}_t$) is chosen as shown in equation (2.1)

$$\hat{\theta}_t = \min_{\theta} \sum_{\tau=1}^{t} (y(t) - \hat{g}(q, \theta)u(t))^2 \qquad (2.1)$$

The optimal parameters are solved using a recursive least-squares algorithm.

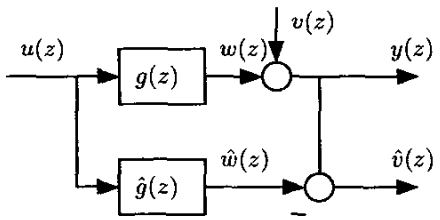

Figure 1: Fullband Identification Block Diagram

The properties of the aforementioned full-band identification method are well understood. It is known [1] that, if $g(z)$ is linear time-invariant and has a finite impulse response with the tap size less than or equal to n_f, then $\hat{g}(z)$ is guaranteed to converge to $g(z)$ asymptotically. From [5], we know that the convergence rate of the parameters is approximated by

$$\mathcal{E}\{\sigma^2_{\tilde{w}(t)}\} \rightarrow \frac{n_f}{t}\sigma_v^2 \; as \; n_f, t \longrightarrow \infty \qquad (2.2)$$

where $\tilde{w}(t) = w(t) - \hat{w}(t)$. The computational cost depends on the particular recursive least-squares (RLS) algorithm used, ranging from $O(n_f)$ to $O(n_f^2)$. Fast algorithms should be used for applications with a high order model, but they tend to be difficult to implement and sensitive numerically; see [6] for a summary of RLS algorithms. For comparative purposes, we consider a reasonably efficient algorithm in [2] for which the computational cost, measured in terms of the number of multiplications per sample, is given by

$$\phi = 9n_f$$

From the quick review above, we can already give some intuition why the subband identification can be advantageous compared to full-band identification. To this end, we consider the three key properties as mentioned above: asymptotic residual error, convergence rate, and computational cost. For simplicity, we assume the critical sampling case where $D = M$. First, we point out that in each subband, the frequency response of the system is much smoother. Therefore, each subband model requires a much lower tap size, compared to the full-band model. It turns out that it is reasonable to take the tap size for each subband model to be n_f/M plus a small constant which we will ignore here. This assures that the subband identification has a negligible asymptotic residual error. Secondly, we note that the number of samples in each subband is reduced by a factor of M. This means that the convergence rate remains roughly the same. Thirdly, the computational cost will be M times cheaper because both the tap size and the number of samples in each subband is reduced by a factor of M and that there are M subbands. For RLS algorithms with complexity more than $O(n_f)$, there will be more savings offered by the subband approach. The analysis above shows clearly the advantage of the subband approach. However, we have not taken into account the extra computation required for forming the subband signals. As we will see later that this is a major design issue which determines the efficiency of the subband approach. Nevertheless, we have seen the possibility of using subbands to save computations.

3 Subband Representation

The subband identification idea is depicted in figure 2. Here $u(z), v(z)$ and $g(z)$ are as in section 2 and we use

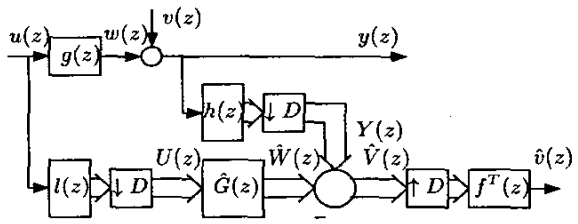

Figure 2: Subband Identification Block Diagram

frequency domain signals every where.

As we mentioned in Introduction, the idea of subband identification is to split both signals $u(z)$ and $y(z)$ into M subbands using two analysis filterbanks $l(z)$ and $h(z)$. These subband signals are down-sampled and the results are denoted by two vector signals $U(z)$ and $Y(z)$. The subband model $\hat{G}(z)$ is identified in order to reconstruct $\hat{W}(z)$ which is the subband equivalent of $\hat{w}(z)$. The

prediction error $\hat{V}(z)$ is then formed. Finally a synthesis filterbank is used to reconstruct $\hat{v}(z)$.
An alternative representation of the subband identification scheme is the polyphase representation depicted in Figure 3. The relationship between the representations

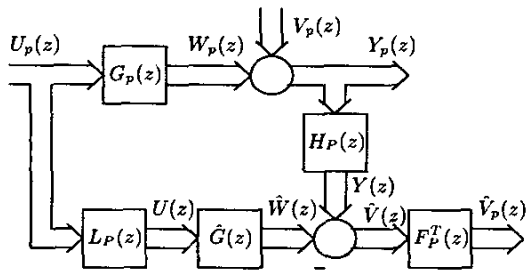

Figure 3: Polyphase Representation of Subband ID

is standard [7] and is given below:

$$G_P(z) = \begin{bmatrix} g^{(0)}(z) & g^{(1)}(z) & \vdots & g^{(D-1)}(z) \\ z^{-1}g^{(D-1)}(z) & g^{(0)}(z) & \vdots & g^{(D-2)}(z) \\ & \cdots & & \\ z^{-1}g^{(1)}(z) & z^{-1}g^{(2)}(z) & \vdots & g^{(0)}(z) \end{bmatrix} \tag{3.1}$$

$$H_P(z) = \begin{bmatrix} h_0^{(0)}(z) & h_0^{(1)}(z) & \vdots & h_0^{(D-1)}(z) \\ h_1^{(0)}(z) & h_1^{(1)}(z) & \vdots & h_1^{(D-1)}(z) \\ & \cdots & & \\ h_{M-1}^{(0)}(z) & h_{M-1}^{(1)}(z) & \vdots & h_{M-1}^{(D-1)}(z) \end{bmatrix} \tag{3.2}$$

where $g^{(i)}(z)$ is the ith polyphase component of $g(z)$, i.e.,

$$g(z) = \sum_{i=0}^{D-1} z^{-i} g^{(i)}(z^D) \tag{3.3}$$

A similar definition applies to $l_k^{(i)}(z)$, $h_k^{(i)}(z)$, etc. The matrix functions $L_P(z)$ and $F_P(z)$ are defined similarly to $H_P(z)$.
It is assumed throughout the paper that $H_P(z)$ and $L_P(z)$ are stable and invertible. The invertibility is required for the subband system to preserve all the information in the full-band.
It is straightforward to verify that the conditions for the subband to have the same representation as the full-band:

$$\hat{G}(z) = H_P(z)G(z)L_P^{-1}(z) \tag{3.4}$$

and

$$F_P^T(z)H_P(z) = z^{-d}I \tag{3.5}$$

where $d \geq 0$ is an integer to allow some delays in the noise estimate $\hat{v}$.

The two analysis filterbanks can be different in which case some frequency shaping of the system model can be achieved. But in this paper, we assume they are the same, i.e., $L_P(z) = H_P(z)$.

4 Decoupling of Subbands

In general, the condition (3.4) requires the subband model $\hat{G}(z)$ to be a full matrix. This complicates the identification process substantially. To simplify the computation, the filterbank $H(z)$ is usually designed to reduce the number of non-zero terms in $\hat{G}(z)$. In the following, we analyze the ideal case where the subband channels are decoupled which implies that $\hat{G}(z)$ is a diagonal matrix.
It is intuitive to see that decoupling of subbands requires each filter $h_m(z), m = 0, ..., M-1$, to have a finite support σ_m. That is, their ideal frequency response is $h_m(e^{j\omega}) = 0$ outside its support. These filters are typically implemented using FIR filters. Since the tap sizes of filters have a negative influence on the computational cost, it is desirable to minimize them. In order to do that, it is required that σ_m be a connected subset of $[-\pi, \pi]$. Decoupling of subbands also implies that σ_m has measure less $2\pi/D$. Finally, (3.4) requires that the union of σ_m equals to $[-\pi, \pi]$. In summary, the supports $\sigma_m \in [-\pi, \pi]$ of the filters $h_m(z)$ need to meet the following conditions:

C1 σ_m is a connected subset of $[-\pi, \pi]$

C2 σ_m has a measure less or equal to $2\pi/D$

C3 $\cup_{m=0}^{M-1} \sigma_m = [-\pi, \pi]$

If $D = M$, these three requirements imply that $h_m(z)$ are simply a set of non-overlapping ideal bandpass filters with the passband having a length of $2\pi/D$. In the case where $D < M$, the filters $h_m(z)$ are still ideal bandpass filters with the same bandpass length, but in this case their supports are allowed to overlap.
To complete this section, we study the tap size n_s required for each subband model. For this we introduce the following result:

Theorem 1 *Consider the subband identification scheme of figure 2. If $l(z) = h(z)$, and $h(z)$ met the three conditions above, then the model required in every subband is given by*

$$\hat{G}_m(t) = (\Gamma_m(\tau) * g(\tau))(Dt) \tag{4.1}$$

where $\Gamma_m(z)$ is the ideal passband filter given by

$$\Gamma_m(\omega) = \begin{cases} 1 & \omega \in \sigma_m \\ 0 & \omega \notin \sigma_m \end{cases}$$

Proof: A sketch of the proof is given below. It is known [7] that

$$x(Dt) = \mathcal{Z}^{-1}\left\{\sum_{d=0}^{D-1} x(W^d z^{1/D})\right\} \qquad (4.2)$$

where $W = e^{j\frac{2\pi}{D}}$, and if $z = r\exp(j\phi)$, then $z^{1/D} = r^{1/D}\exp(j\frac{mod(\phi,2\pi)-\pi}{D})$. Let $W(z)$ be the subband equivalent of $w(z)$, then

$$\begin{aligned} W_m(z) &= \frac{1}{D}\sum_{d=0}^{D-1} h_m(W^d z^{1/D}) g(W^d z^{1/D}) u(W^d z^{1/D}) \\ \hat{W}_m(z) &= \hat{G}_m(z)\frac{1}{D}\sum_{d=0}^{D-1} h_m(W^d z^{1/D}) u(W^d z^{1/D}) \end{aligned}$$

Let $\beta_m(z) = V^{-m}(V^{Dm}z)^{1/D}$ with $V = e^{j\frac{2\pi}{M}}$ (i.e. $\beta_m(z)$ maps the unit circle into the support of the filter $h_m(z)$). It can be shown that the two equations above are still true if we replace $z^{1/D}$ by $\beta_m(z)$. Doing this and taking into account that $h_m(W^d\beta_m(z)) = 0$ $(d = 1, ..., D-1)$, if we want $W_m(z) = \hat{W}_m(z)$, we need

$$\hat{G}_m(z) = g(\beta_m(z)) \qquad (4.3)$$

On the other hand, from (4.2), we have that

$$(\Gamma_m(\tau) * g(\tau))(Dt) = \mathcal{Z}^{-1}\{g(\beta_m(z))\} \qquad (4.4)$$

since $\Gamma_m(W^d\beta_m(z)) = 0$ $(d = 1, ..., D-1)$. Equation (4.1) follows immediately from equations (4.3) and (4.4). ∎

Taking $h(z) = l(z)$ and using (4.1), we can choose

$$n_s = \frac{n_f}{D} + n' \qquad (4.5)$$

where n' is the amount of extra parameters required due to the spread that the convolution produces on $g(\tau)$. For most applications where high accuracies are not required, it is usually sufficient to choose a small n'. Typically, $n' < 20$.

5 Critical-Sampling Case

In the case of critical sampling, $D = M$. The decoupling condition implies that each support σ_m is connected and has measure equal to $2\pi/D$. However, the shape of each filter $h_m(z)$ within its support determines the convergence rate of the corresponding subband model. It can be shown that, in order to maximize the convergence rate, $h_m(e^{j\omega})$ needs to be flat within its support. Consequently, the ideal analysis filterbank is given by

$$\begin{aligned} h_m(z) &= h_0(V^m z) \quad (m = 0, ..., M-1) \\ |h_0(e^{j\omega})| &= \begin{cases} \sqrt{D} & -\frac{\pi}{M} < \omega < \frac{\pi}{M} \\ 0 & \text{otherwise} \end{cases} \end{aligned} \qquad (5.1)$$

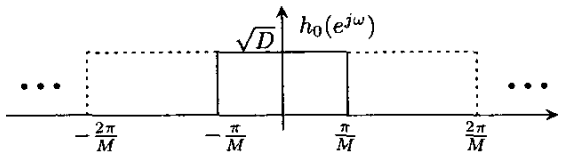

Figure 4: Analysis filterbank choice for the critical-sampling case

The filterbank is depicted in Figure 4. This conclusion is actually a special case of theorem 2 in section 6.

The ideal filters $h_m(z)$ will be approximated using linear phase FIR filters of length l, whose frequency response can not have zero amplitude in its stopband. Suppose u is a white random process and we want to minimize the error due to interference in between subbands. It can be shown that the FIR filter should be the one that minimizes the energy (λ) in its stopband. This filter is known to be an FIR eigenfilter; see [8]. The required tap size $l(M, \lambda)$ can be computed numerically. The choice of λ influences the asymptotic residual error for the subband identification. Hence, λ needs to be small. However, λ should not be too small or the filtering cost will be too high.

Once the analysis filterbank is determined as above, the synthesis filter is a dual filterbank. In theory, the filters of the dual filterbank have infinite length, but empirical results show that they can be truncated up to the same length as the analysis filters without having a significant reconstruction error. Hence, the computation for the synthesis filterbank is compatible to that for an analysis filterbank.

It is easy to see that with the filterbank design (5.1), the convergence rate is given by

$$\mathcal{E}\{\sigma^2_{\tilde{w}(t)}\} \to \frac{n_s}{t/D}\sigma_v^2 \simeq \frac{n_f}{t}\sigma_v^2 \; as \; n_s, t \longrightarrow \infty \qquad (5.2)$$

which coincides with (2.2). Finally, the computational cost needs to include the overhead for computing the subband signals $U(z)$ and $Y(z)$ and reconstruction of $\hat{v}(z)$, and is given by

$$\phi = 3l(M, \lambda) + 9n_s \simeq 3k(\lambda)M + 9\frac{n_f}{M} \qquad (5.3)$$

where the approximation corresponds to the case where $n_f \gg n'$. From (4.5), (5.2) and (5.3), it is clear that we can optimize the value of M so as to minimize the computational cost while having the asymptotic residual error and convergence rate compatible with the fullband method.

6 Oversampling Case

The case of critical sampling has the obvious advantage that the number of subbands is minimal. This is cer-

tainly a factor that influences the computational cost. The disadvantage of critical sampling is that the filters $h_m(z)$ need a sharp transition band. The required filter length is considerably long, which contributes negatively to the computational cost. The idea of oversampling is to increase the value of M so as to allow filter patterns that are easier to approximate using FIR filers.
In a way similar to section 5, we want to design $h_m(z)$ to yield fast convergence rate. We have the following result to this end.

Theorem 2 *Consider the filterbank design for the oversampling case where $D \leq M$. The filters $h_m(z)$ are required to satisfy the conditions C1-C3. Then, in order to maximize the convergence rate, the best choice for the analysis filterbank is given by*

$$h_m(z) = h_0(V^m z) \quad (m = 0, ..., M-1) \qquad (6.1)$$

$$|h_0(e^{j\omega})| = \begin{cases} \sqrt{D} & -\omega_1 < \omega < \omega_1 \\ \sqrt{\frac{D}{\omega_2 - \omega_1}}\sqrt{\omega_2 \mp \omega} & \pm\omega_1 < \omega < \pm\omega_2 \\ 0 & \omega_2 < |\omega| < \pi \end{cases}$$

where $\omega_1 = 2\pi\left(\frac{1}{M} - \frac{1}{2D}\right)$ and $\omega_2 = 2\pi\left(\frac{1}{2D}\right)$. The filter shape is depicted in Figure 5.

Proof: To be provided in the full version of the paper. ■

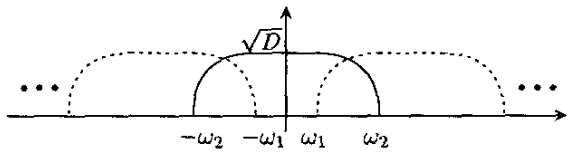

Figure 5: Analysis filterbank choice for the oversampling case

As in section 5, we will approximate the ideal filters $h_m(z)$ with linear phase FIR eigenfilters. The tap size of the filter will be denoted by $l(M, D, \lambda)$, where λ is the energy difference between the ideal filter and the FIR eigenfilter. Again, the tap size can be determined numerically.
With the filter design (6.1), the convergence rate coincides with (5.2). The computational cost is given by

$$\phi = \frac{M}{D}(3l(M, D, \lambda) + 9n_s) \qquad (6.2)$$
$$\simeq \frac{M}{D}(3l(M, D, \lambda) + 9\frac{n_f}{D})$$

We can numerically optimize the values of M and D to give the minimum computational cost.

7 Simulation Results

In sections 5 and 6, we state that, with the two cases of the subband method, we can have the same performance as the fullband method (asymptotic residual error and convergence rate) at less computational cost. Further, we expect that the computational savings are more significant in the oversampling case. In order to illustrate this, we identified the transfer function of figure 6 using the tree methods.

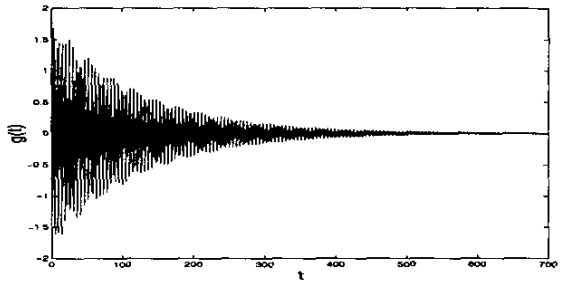

Figure 6: Plant Impulse Responce

We used a tap size of $n_f = 200$ for the fullband method. This choice of n_f means that the full band model ignores the part of the impulse response after $t = 200$, resulting approximately 6% of error. The tap size of each subband model will depend on the value of D, as shown in equation (4.5). We take $n' = 1$ which is sufficient for the subband method to have a compatible error.
As said before, either equation (5.3) or (6.2) needs to be numerically minimized in order to get the optimal values of M and D. In figure 7 we show the computational cost as a function of M. To plot the oversampling case, the computational cost corresponds to that obtained by using the optimal value of D for each M. From the figure, it looks like the computational cost of the oversampling case remains constant after $M \simeq 10$; however, for $M > 20$ it grows again. For this example, the adopted values are $M = 3$ for the critical-sampling case and $M = 15$, $D = 11$ for the oversampling case.
In the design of the filterbanks, the adopted value of the leakage energy was $\lambda = 0.05$. The filterbanks for both cases can be seen in figures 8 and 9. The evolution of the power of the identification error is shown in figure 10. We see that the convergency rate and residual error of the three methods are compatible. However, the computational costs are 1800 multiplications per (fullband) sample. for the fullband method, 1002 for the critical-sampling subband method and 452 for the oversampling subband method.

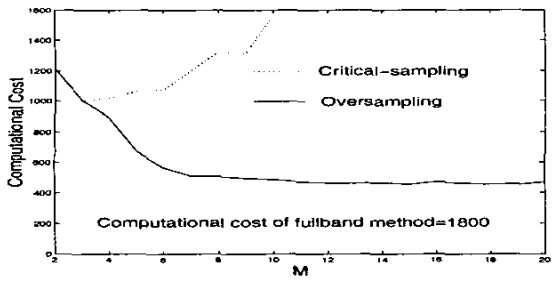

Figure 7: Computational Cost vs. M

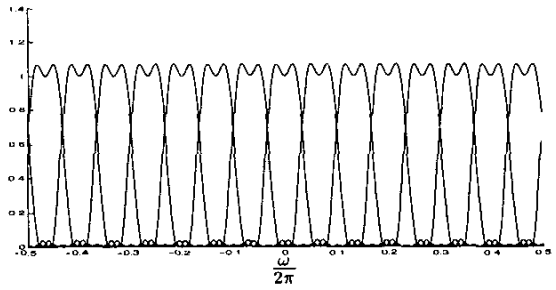

Figure 9: Filterbank for the oversampling case

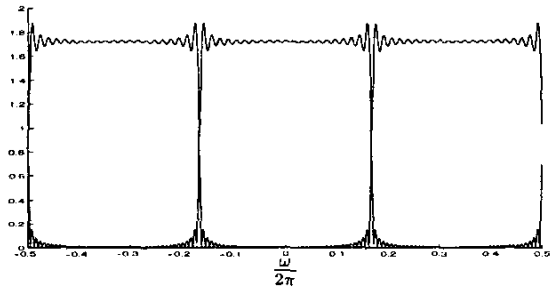

Figure 8: Filterbank for the critical-sampling case

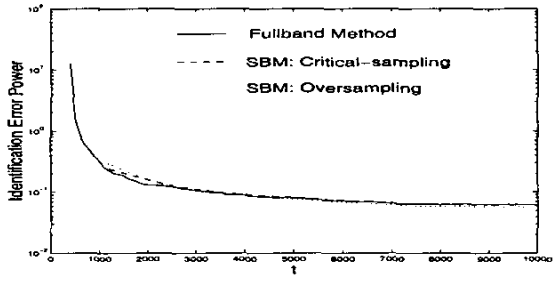

Figure 10: Evolution of the identification error power

8 Conclusions

In this work, we have analyzed the performance of the decoupled subband identification method, in both critical-sampling and oversampling cases, by comparing them with the classical time-domain identification method (the fullband method). The comparison is based on three performance indexes: computational cost, convergence rate and asymptotic residual error.
In sections 5 and 6, and equation (4.5), we have shown that, with the appropriate design of the filterbanks, and the appropriate selection of the number of parameters in each subband, the convergence rate and asymptotic residual error of both subband methods are compatible with that of the fullband method, but, if the impulse response of the system to be identified is large enough, the computational costs are smaller. Further, more computational savings are expected in the oversampling case since it includes the critical-sampling case as a particular case.

References

[1] Lennart Ljung, *System Identification: Theory for the User*, Prentice Hall, second edition, 1999.

[2] M. L. Honing and D. G. Messerschmit, *Adaptive Filters: Structures, Algorithms, and Applications*, Boston: Kluwer, 1984.

[3] Andre Gilloire and Martin Vetterlli, "Adaptive filtering in subbands with critical sampling: analysis, experiments, and application to acoustic echo cancellation," *IEEE Transactions on Signal Processing*, vol. 40, no. 8, pp. 1862–1875, August 1992.

[4] Youhong Lu and Joel Morris, "Gabor expansion for adaptive echo cancellation," *IEEE Signal Processing Magazine*, pp. 68–80, March 1999.

[5] Lennart Ljung and Zhen-Dong Yuan, "Asymptotic properties of black-box identification of transffer functions," *IEEE Transactions on Automatic Control*, vol. AC-30, no. 6, pp. 514–530, June 1985.

[6] John G. Proakis, Charles M. Raider, Fuyun Ling, and Chrysostomos L. Nikias, *Advanced Digital Signal Processing*, Maxwell Macmillan International, 1992.

[7] P. P. Vaidyanathan, *Multirate Systems and Filterbanks*, Prentice Hall, 1993.

[8] Damian Marelli and Minyue Fu, "Optimized filterbank design for subband identification with oversampling," in *Proceedings of the 26th International Conference on Acoustics, Speech, and Signal Processing (ICASSP)*, 2001.